RSC Advances

PAPER

View Article Online
View Journal | View Issue

Cite this: *RSC Adv.*, 2019, **9**, 7818

Validation of 'lock-and-key' mechanism of a metal–organic framework in selective sensing of triethylamine†

Kowsalya Vellingiri,[a] Danil W. Boukhvalov,[bc] Ki-Hyun Kim[d] and Ligy Philip *[a]

Received 29th December 2018
Accepted 4th March 2019

DOI: 10.1039/c8ra10637a

rsc.li/rsc-advances

To develop the metal–organic framework (MOF)-based sensing of triethylamine (TEA) in an aqueous phase, Al-MIL-101-NH_2 (MIL: Material Institute Lavoisier) with a tripod-like cavity was utilized based on a lock-and-key model. Al-MIL-101-NH_2 (Al-MOF) was found to be an excellent fluorescent sensor for the TEA molecules in the range of 0.05–0.99 mM. The limit of detection (LOD) and linear calibration range of this probe towards TEA were found to be 3 μM and 0.05–0.40 mM, respectively. The mechanism of the sensing process indicates the dominant role of physical processes (*e.g.*, non-covalent bond interactions). In addition, the exact fit of the TEA molecule (6.5 Å) in the tripod-like cavity (6.78 Å) supported the strong interaction between three ethyl groups (TEA) and aromatic rings (MOF). This kind of specific suitability between size/shape of the TEA and tripod-like cavity of MOF (ΔG: −46.7 kJ mol^{-1}) was not found in other molecules such as ethylamine (ΔG: −2.20 kJ mol^{-1} and size: 3.7 Å), formaldehyde (ΔG: +1.50 kJ mol^{-1} and size: 2.8 Å), and ammonia (ΔG: +0.71 kJ mol^{-1} and size: 1.6 Å). As such, Al-MOF was found to be a selective and stable sensor for TEA.

1. Introduction

Triethylamine (TEA) is a well-known raw material for catalysis and condensation reactions or as a preservative that is scalable to industrial applications.[1,2] Apart from such common applications, it acts as a curing agent for the hardening of polymers.[3] Because of the extended use, many industrial wastewaters/flue gasses contain traces or significant concentrations of TEA. TEA discharged into the environment is toxic, volatile, and flammable and is a threat to the environment and humans.[4] For instance, the acute exposure of TEA is reported to cause eye/skin/mucous membrane irritation, and corneal swelling.[5,6] Thus, accurate monitoring of this toxic pollutant in the hood and discharge units of industries is now considered a major concern with respect to environmental management.

To date, the detection of TEA has generally been carried out by gas sensing devices and/or conventional instrumental methods.[7,8] However, the analytical procedures based on the latter (*e.g.*, sampling and pre-concentration) were time consuming and require sophisticated instruments (*e.g.*, gas chromatography). Therefore, it is important to create portable but sensitive analytical methods such as sensor. In this regard, several types of sensors including optical,[9] semiconductor,[10] electrochemical,[11] and luminescent sensors[12,13] have been developed and employed for the sensing of TEA in vapour phase. In contrast, studies related to the sensing of TEA in aqueous phase are minimal.

In an effort to create a sensor for aqueous phase detection of TEA, wide range of nanomaterials with superior advantages (*e.g.*, easy turn on-turn off sensing ability, reliability of luminescence intensity, and accessible porosity) have been developed.[12] Among those materials, metal oxides, quantum dots (QD), graphene oxide (GO), and metal–organic frameworks (MOFs) were mostly preferred for the detection of small volatile organic molecules (VOCs). Here, MOFs are the coordination polymer which possesses high surface area, pore volume, enlarged structural flexibility, stable luminescent property, and high thermal and aqueous stability.[14–16] It has been envisioned that ligand molecules are responsible for the luminescent property of the MOFs. In this context, diverse luminophores (such as $–NH_2$, SO_3^-, and –OH) have been used to prepare MOFs with Lewis acidic/basic sites.[17,18] These luminophores can produce strong fluorescence properties to help enhance the sensitivity of the MOF.[19] In some cases, along with the support from functional groups, cavities, and pore size of the MOFs also considered as an efficient active sites for sensing of small organic molecules. In this respect, the cavities of luminescent microporous MOFs and chiral porous MOFs were found to

[a]*Environmental and Water Resources Engineering Division, Department of Civil Engineering, IIT Madras, Chennai 600 036, India. E-mail: ligy@iitm.ac.in*

[b]*College of Science, Institute of Materials Physics and Chemistry, Nanjing Forestry University, Nanjing 210037, P. R. China*

[c]*Theoretical Physics and Applied Mathematics Department, Ural Federal University, Mira Street 19, 620002 Yekaterinburg, Russia*

[d]*Department of Civil and Environmental Engineering, Hanyang University, 222 Wangsimni-Ro, Seoul 04763, Korea*

† Electronic supplementary information (ESI) available. See DOI: 10.1039/c8ra10637a

provide an exact fit for the aromatic explosives,[20] dyes,[21] and amino alcohols.[22] The bonding of molecules packed in the cavities/pores was mainly accompanied by weak interactions such as hydrogen bonding.[22] This kind of structural advantages of MOFs was however, not widely utilized especially in the field of luminescent sensing of small molecules.

In this research, the structural property (*e.g.*, cavity size) of Al-MIL-101-NH_2 (Al-MOF) was utilized for the sensing of TEA in an aqueous solution. Al-MOF has large pores (*ca.* 3.4 nm) and two types of cavities; one wider corner like cavity (10.39 Å) and the other with narrower tripod like cavity (6.78 Å). Tripod-like shapes are commonly used for the preparation of multiple interpenetrated frameworks.[23] In this work, the size of tripod like cavity (6.78 Å) of Al-MOF was found to be exactly sufficient to fit TEA molecule (6.50 Å). This exact fitting was similar to the mechanism of lock-and-key model. More specifically, tripod like concave is suspected to act as a lock to offer exact fit for incoming TEA molecule (key) (Scheme 1). This kind of lock-and-key model was common in supramolecular chemistry field while the use of this mechanism for the sensing of small molecules has not been reported from any studies to date. Thus, this study proved the specific size induced mechanism of Al-MOF towards TEA through experimental as well as theoretical results.

2. Experimental methods

2.1. Laboratory synthesis of Al-MOF

The preparation procedure of Al-MOF was adopted from the study conducted by Xu and Yan[24] after some minor modifications. The detailed synthesis procedure along with the information about chemicals and instruments used for characterization analysis are provided in ESI (ESI: Section 1.1–1.3†). The procedure used to test the stability of Al-MOF with respect to ambient storage (day-to-day stability) and temperature is also provided in Section 1.4–1.5 of ESI.†

2.2. Sensing and selectivity profiles of Al-MOF against triethylamine

Initially the fluorescent behaviour of ligand and MOF was investigated. For this measurement, 3 mL of ligand/MOF probe solution was kept in a quartz cuvette to monitor their emission spectrum. Secondly, the sensing efficiency of Al-MOF was investigated against diverse concentration of TEA solution at room temperature (RT). Here, standard solutions of TEA prepared at different concentrations were added (20 μL) into the quartz cuvette containing 2 mL of Al-MOF solution. Final concentration of TEA solution was maintained in the range of 0.50–0.99 mM. After each addition of TEA, the fluorescent spectrum was immediately monitored. The effect of temperature on the sensing behaviour of Al-MOF was investigated. Selectivity of Al-MOF towards TEA was studied in the presence of other ethylamines and low molecular weight organic compounds in single and multiple species levels (refer to Section 1.6 of ESI†). All the measurements were conducted in triplicate. Their average values were used to present the fluorescent sensing behaviour of Al-MOF against TEA.

2.3. Theoretical modelling studies

Modelling studies related to sensing mechanism of Al-MOF was estimated by density functional theory (DFT) calculations. The detailed description about the calculation was presented in the Section 1.7 of ESI.†

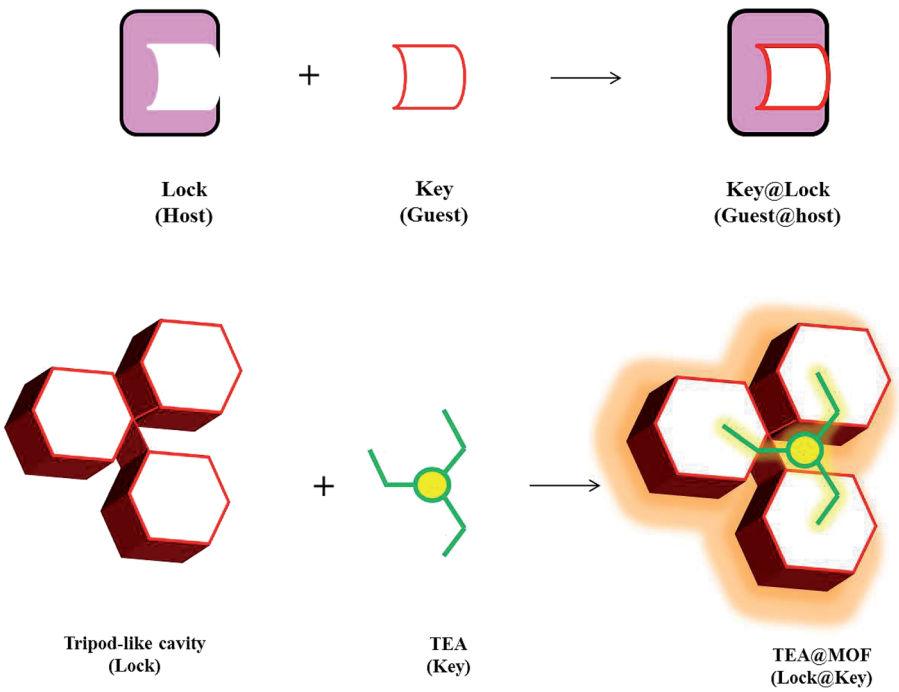

Scheme 1 Proposed lock-and-key mechanism for the sensing of TEA using Al-MOF.

3. Results and discussion

3.1. Characterization

Results of PXRD analysis confirmed the crystalline nature of Al-MOF especially in the 2θ region of $2-20^\circ$ (Fig. S1a†). The obtained PXRD spectrum was comparable to the simulated PXRD pattern of MIL-101 framework.[25] It should be noted that a slight shift of the peaks in the 2 theta region of 2–6° indicate a minor deviation in the lattice parameter of synthesized Al-MIL-101-NH_2 (*e.g.*, 2 theta $\sim 1/3 \times a^2$). This decrease in the lattice parameter might have originated from the presence of amorphous impurities in the crystalline structure of Al-MOF.[26] Apart from this slight deviation in lattice parameter, all other specific features related to $Fd\bar{3}m$ space group were clearly observed in the PXRD pattern of Al-MOF. The FTIR bands located in the region of ~3400–3300 cm^{-1} were associated with free and unassociated $-NH_2$ group of Al-MOF (Fig. S1b†). In addition, the presence of strong band at 1577, 1435, and 1084 cm^{-1} indicated –C–N stretching vibrations. Evident three peaks in the region of 1620, 1582, and 1468 cm^{-1} confirmed the presence of –N–C and C═O interaction (Fig. S1c†). The morphology of the synthesised Al-MOF was found to be aggregated crystals of different shapes and sizes (Fig. S1d†). This obtained morphology was different with previously seen morphology *i.e.*, needle-shaped flower like aggregated crystals.[24] This discrepancy in morphology was mainly rose from the adopted different drying process. BET (S_{BET}) and Langmuir surface area of the synthesized Al-MOF was 276 and 410 $m^2\ g^{-1}$, respectively (Table S1† and Fig. S2a†). The obtained surface area was smaller than the reported surface area by Xu and Yan[24] (422 $m^2\ g^{-1}$). This difference in the surface area might be due to the rate of addition of Al-component to the reaction mixture.[26] In the present study, the rate of addition of $AlCl_3 \cdot 6H_2O$ was faster (5 min intervals) than the one employed by Xu and Yan[24] (10 min intervals). This fast addition of Al-component might have influenced the surface area of the Al-MOF and this is the only limitation of the present synthesis route. The pore size distribution curve of Al-MOF is shown in Fig. S2b.† The calculated adsorption and desorption average pore diameter ($4V/A$) were 0.17 and 0.13 nm, respectively (Table S1†). The calculated molecular formula of Al-MOF is $Al_3O(DMF)(BDC\text{-}NH_2)_3 \cdot nH_2O$. TGA analysis of Al-MOF was shown in Fig. S2c.† The loss of 10.7% was observed around 100–120 °C correspond to the coordinated water molecules. Secondly, the mass loss of 6.2% in the region of 150–180 °C was responsible for the elimination of coordinated DMF and weight loss of about 10.5% in the temperature region of 250–400 °C was corresponding to the decomposition of BDC-NH_2. The final weight loss observed after 470 °C (27.1%) was corresponding to the formation of Al_2O_3. To this end, Al-MOF was stable up to the temperature of 470 °C (Fig. S2c†).

3.2. Luminescent property of Al-MOF

Optical property of Al-MOF was investigated through UV-Visible spectroscopy measurement. The amino portion of the MOF was responsible for the electronic charge transfer ($\pi \rightarrow \pi^*$). Thus, it is important to first study the optical properties of BDC-NH_2. The emission spectrum of BDC-NH_2 showed a weak and broad absorption at 400 nm (Fig. S3a†).[24] Likewise, Al-MOF was also showed similar absorbance behaviour. In contrast, the acquired absorption value was ~two times larger than ligand molecule. The maximum fluorescence intensity (λ_{em}) at 450 nm was observed when λ_{ex} was fixed as 396 nm (Fig. S3b†). This result indicates the efficient charge transfer between the ligand and open metal sites of Al (Al^{3+}). This charge transfer phenomenon between MOF and ligand was further confirmed by the calculation of Mulliken occupancies.

In a simple system, the interaction of molecules with any surfaces can be evaluated by integrating the charge densities along the chosen axis.[27] In contrast, in a complex (sophisticated) system like MOFs, the change in charge densities can be estimated with the help of Mulliken occupancies (*i.e.*, the sum of electrons over valence orbitals) on Al^{3+} ions. The charge density measurement also confirmed an increase in the Mulliken population around the Al^{3+} centres (about 0.29 e^- per Al^{3+} centre). Such increase may provide evidence that the significant charge transfer should have taken place[27] (refer to Section 2.1 of ESI†). It should be noted that the calculation of exact Mulliken occupancies for Al^{3+} ions was difficult because of the frequent electron moment and corresponding difference in radii of atomic spheres of Al^{3+} ions.

Fluorescent probe showed enhanced day-to-day stability in an aqueous phase (Fig. S4a†) *i.e.*, there was no considerable change in fluorescent intensity of probe over 7 days (*e.g.*, relative fluorescence unit (RFU) of day-1 and day-7 was 241 and 250 a.u.). This stability was mainly obtained from the metal centre and partially contributed by the $-NH_2$ group present in the MOF[28] and it was also confirmed by Gibbs free energy calculation of MOF.

3.3. pH dependent property of Al-MOF

TEA is a basic organic amine with the pK_b value of 4.75. Therefore, even a small amount of TEA in water can increase the pH of the solution rapidly. So, the pH effect of Al-MOF at different pH conditions was studied. The result indicated that as pH increases the RFU value of MOF was also increased (Fig. S5†). This kind of behaviour was already reported by Xu and Yan.[24] In their study, the fluorescent intensity of Al-MOF was increased when pH increased from 4 to 7.7 and the result of Fig. S5† was in accordance with the results of Xu and Yan.[24] However, further increase in pH of the MOF suspension to 10 lead to the hypsochromic shift (pH-7: 445 nm and pH-10: 430 nm). This result clearly indicates that at basic condition the band gap between highest occupied molecular orbital (HOMO) and lowest unoccupied molecular orbital (LUMO) of Al-MOF was increased about 0.16 eV and resulted the hypsochromic shift of Al-MOF.

Although TEA tends to increase the pH of the system, this kind of hypsochromic shift was not noticed while sensing of TEA by Al-MOF (Fig. 1a). This can be explained based on the charge transfer characteristics of Al-MOF and TEA. The interaction of Al-MOF with reaction medium (water) leads to the formation of donor–acceptor bonds. TEA acts as an acceptor while interacting with Al-MOF whereas it acts as donor when

interacts with water. Therefore, the interaction of Al-MOF with TEA also forms donor–acceptor bonds. It should be noted that these donor–acceptor bonds were highly sensitive towards the change in the pH of the system.

The calculations demonstrated that charge transfer of 0.21 e^- from MOF to TEA was occurred when Al-MOF was used as a TEA sensor. This provides the decreasing of HOMO–LUMO gap of Al-MOF about 0.2 eV that compensate for the increase in band gap caused by basic environment and eliminate hypsochromic shift. On the other hand, the structural properties of Al-MOF also found to be responsible for the absence of hypsochromic shift. For instance, the water molecules preferred to strongly interact with nitrogen centres of Al-MOF, and metal clusters Al-MOF were found to interact with hydrophobic branches of TEA. Consequence of these simultaneous interactions, the excited electrons from basic media is partially removed by Al-MOF that eliminate hypsochromic shift. Therefore, it is possible to utilize Al-MOF as a TEA sensor for a wide range of pH.

3.4. Sensing of triethylamine

3.4.1. Sensing of TEA using Al-MOF. The sensing behaviour of Al-MOF probe against TEA was monitored by visualizing change in fluorescence efficiency of the probe with subsequent addition of TEA. Accordingly, after each addition a considerable increase in the fluorescence efficiency was noticed (Fig. 1a). For instance, the initial RFU of Al-MOF probe was 338 a.u., whereas addition of 0.49 mM of TEA increased the fluorescence efficiency of the original material to 2289 a.u. This enhanced fluorescence was ascribed from favourable electron transfer between MOF and incoming TEA molecule. In addition, it was also observed that after each addition, there was an immediate increase in the fluorescence intensity (within 25 s) of Al-MOF. This immediate response confirms that there was no necessity for the specific incubation time.

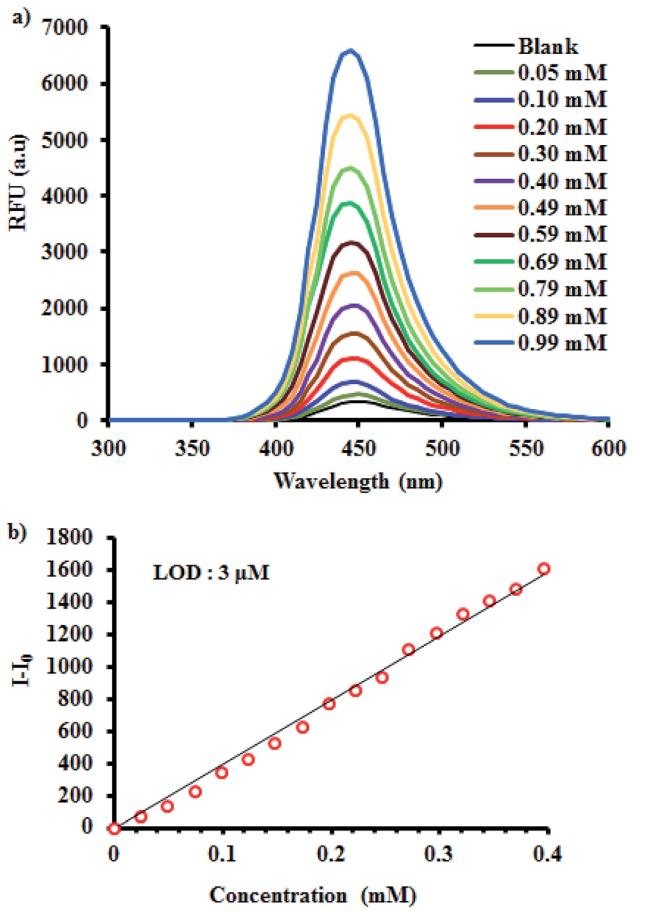

Fig. 1 Fluorescent sensing of TEA using Al-MOF. (a) Emission spectra of Al-MOF at different TEA concentrations and (b) linear calibration plot of Al-MOF with respect to TEA.

In this line, it is also important to check the linear response range of proposed probe because this determines the extension of the application of this material into real field. Accordingly, gradual increase in the fluorescence of Al-MOF against diverse concentration (0.05–0.40 mM) of TEA was observed. Further addition of TEA leads to the polynomial behaviour. The observed linear range yielded a regression coefficient (R^2) value > 0.99 (Fig. 1b). More importantly the structure of the probe was not disturbed with respect to the ambient storage (Fig. S4b–d: Section 2.2 of ESI†) and the probe showed similar sensing performance towards TEA even after a one month at ambient condition (Fig. S6; refer to Section 2.3 of ESI†). In addition, the sensing ability of Al-MOF was not affected by temperature range of RT-60 °C (Fig. S7; Section 2.4 of ESI†). Furthermore, limit of detection (LOD) of Al-MOF was calculated. For this measurement, TEA solution with the final concentration of 0.01 mM was added into probe solution to monitor changes in fluorescence intensity from three subsequent additions. Later, the LOD was calculated using the formula,[14,29]

$$\mathrm{LOD} = \frac{3 \times \sigma}{\text{sensitivity}}$$

where σ is the standard deviation of fluorescent intensity of Al-MOF at triplicate addition of 0.01 mM of TEA and sensitivity is the slope value of I–I_0 plot. From this measurement, the estimated LOD value of Al-MOF against TEA was 3 µM. The obtained LOD value of Al-MOF was far better than those of Filippo *et al.*[30] (1.7 mM). Filippo *et al.*[30] have used colorimetric sensing method for the detection of TEA (0.5 to 50 mM) using sucralose-capped silver nanoparticles. In the course of this analysis, the color of nanoparticles was changed from pale yellow to gray.[30] In comparison with that study, we have achieved much lower LOD (*i.e.*, 3 µM). Additionally, the excellent selectivity along with the good reversibility of the proposed probe (*e.g.*, compared to their colorimetric probe) confirms the suitability of this material for the luminescent sensing of TEA in aqueous phase. Thus, it can be concluded that Al-MOF was found to be a good sensor for aqueous phase TEA.

3.5. Selectivity of Al-MOF towards triethylamine over other analytes

The result of selectivity for the case of single component analysis provides clear evidence that except TEA all other molecules showed much lesser sensitivity towards Al-MOF. For instance,

0.49 mM addition of TEA registered $I–I_0$ value of 2378 whereas all other tested pollutants were in the range of only −40 (FA) to 89 (Py) (Fig. 2a). It is noteworthy to mention that, the negative value of FA was due to its fluorescence quenching nature.[14] Similar results were observed when the selectivity of the probe against TEA was investigated in mixed pollutant condition. As shown in Fig. 2a, there was not much difference between the $I–I_0$ value of TEA and subsequent addition of other pollutants to the probe. This indicates high selectivity and stable fluorescent nature of Al-MOF against TEA. This kind of selective fluorescence behaviour of Zr-based MOFs was also found in our previous studies.[14,15] In order to further confirm the fluorescence enhancement with respect to TEA, 0.49 mM of TEA was additionally added to the reaction mixture. Immediate rising in the fluorescence intensity of Al-MOF was exactly twice of the value obtained in the first addition (Fig. 2a). This increase in fluorescence ensures the selective identification of the TEA by Al-MOF even with other co-existing compounds.

Above result clearly indicated the high selectivity of Al-MOF over other co-existing pollutants. However, the behaviour of Al-MOF with other amines such as EA and DEA is not known. Hence, the selectivity profile of Al-MOF against variety of amines was investigated. Surprisingly, the MOF also showed enhanced fluorescent response for the TEA over other ethylamine in both single and mixed pollutant levels. For instance, Al-MOF was not sensitive towards EA while the addition of DEA enhanced the fluorescence intensity by small quantity (Fig. 2b). Nonetheless, this value was half of the fluorescence intensity of TEA. This observation indicates that increase in the number of ethyl group increased the fluorescence intensity of Al-MOF. Further, in mixed pollutant condition there was no change in the fluorescence efficiency of Al-MOF@TEA even after sequential addition of DEA and EA to the probe (Fig. 2b). This clear cut observation again confirms the ideal selection of TEA molecules by Al-MOF. Enhanced selectivity of the Al-MOF might have resulted from their size and shape related properties of host and guest.

3.6. Sensing mechanism

3.6.1. Characterization analysis. The sensing mechanism was assessed with the help of FTIR characterization of Al-MOF before and after interaction with TEA. The obtained results indicate high structural integrity of the material even after interaction with 0.49 mM of TEA. For instance, the peak responsible for the $–NH_2$ stretching at 3456 and 3384 cm^{-1} was found in both materials. In addition, there was no change in the peak positions of aromatic (Ar.) ring, aryl C–O, –CH, and NC_3 in-(i.ph)/on-phase (o.ph.) stretching vibrations were observed. More importantly, the peaks present at 1497 and 1258, and 774 cm^{-1} corresponds to the stretching frequencies of –N–C bond. The presence of these IR bands confirms the formation of non-covalent bond interactions which is in accordance with the DFT calculations (Fig. S8†). Additionally, a slight increase in the intensity of IR bands at 1258 and 774 cm^{-1} confirms the effective charge transfer between Al-MOF and TEA through donor–acceptor interactions. In order to further confirm the crystalline stability of MOF after interaction with TEA, PXRD and FTIR analysis was performed (Fig. S9 and S10†). Both the analysis, no distinctive change in the crystalline structure and chemical nature of the MOF was observed. These results indicate that the structure of MOF was intact towards the incoming TEA molecule. Overall characterization analysis suggests that

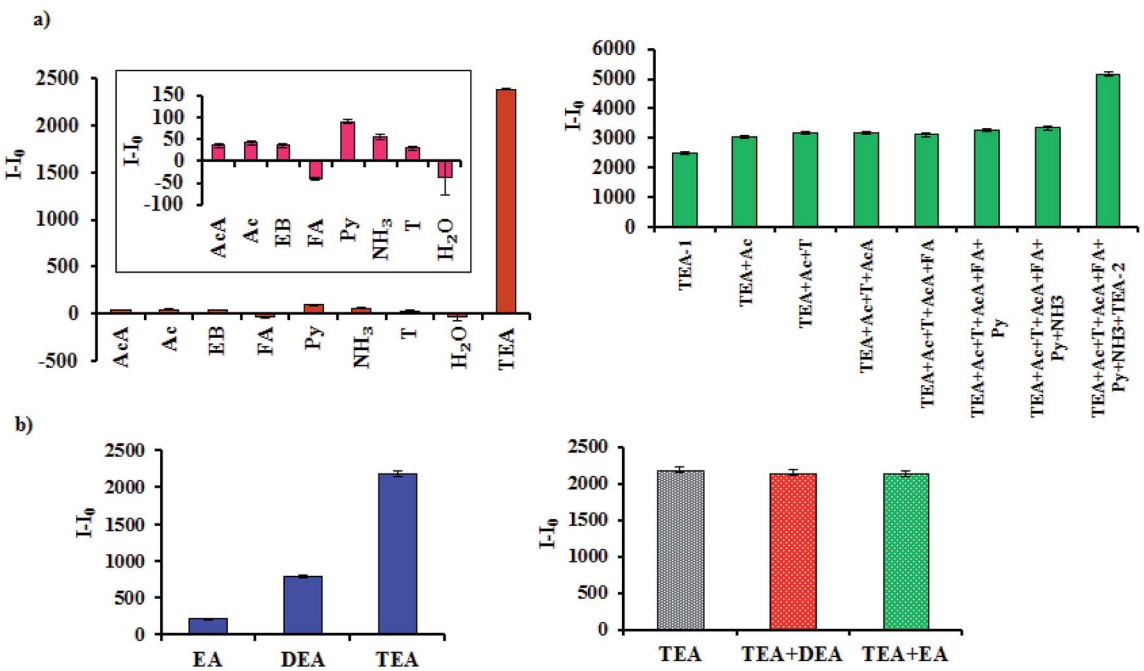

Fig. 2 The selectivity profile of Al-MOF towards TEA with common co-existing pollutants (a) and family of ethyl amines (b) (MOF and pollutant concentration: 1 g L^{-1} and 0.49 mM, respectively).

sensing of TEA using Al-MOF should be due to non-covalent bond interactions.[14] Although, this kind of interactions was generally weaker than van der Waals interactions, the cumulative interaction of these small forces finally results stronger impact on the fluorescence behaviour of Al-MOF.

3.6.2. DFT calculations. Results of DFT calculations demonstrated that the interaction of one ethyl group of TEA with linker portion of Al-MOF was less strong than interaction of FA and NH_3 molecules with same linker. In contrast, TEA-molecule could interact simultaneously with three aromatic rings of MOF (Fig. 3) and this kind of multiple interaction sites was not possible in small molecules. Thus, the magnitude of adsorption enthalpy of TEA was significantly larger ($\Delta H_{(water)} = -81.7$ kJ mol^{-1}) than FA (-31.9 kJ mol^{-1}) or NH_3 (-22.3 kJ mol^{-1}) (Table 1). This enhanced $\Delta H_{(water)}$ value of TEA–MOF interaction can be explained based on the structural relationship between guest and host. In detail, among the two different cavities (*e.g.*, corner-like and narrower tripod-like cavities) in Al-MOF, the latter was found to provide an exact fit for the TEA molecule as seen in Fig. 3. Contrastingly, for sensing of FA or NH_3 shape of the cavities plays a minor role. This is because they interact with only one aromatic ring of linker and finally these molecules were escaped from the cavities.

The formation of bond between Al-MOF and TEA creates an increase in the energy cost for the rotation of aromatic rings in Al-MOF. For instance, before interaction with TEA, the energy cost for the rotation of single aromatic ring at 10° was about 5 kJ mol^{-1}. On the other hand, after interaction with TEA it was observed to increase up to ~20 kJ mol^{-1}. The construction of

Table 1 Summary of enthalpy of adsorption, Gibbs free energy (kJ mol^{-1}), size, and distances (in Å) between molecules and MOFs

Molecule	Size	$\Delta H_{(air)}$	$\Delta H_{(water)}$	ΔG	Distance
(a) Amines					
TEA	6.5	−120	−81.7	−46.7	C–H 2.92
					H–H 2.35
DEA	6.0	−95.2	−51.6	−20.5	C–H 2.99
					H–H 2.67
EA	3.7	−59.2	−30.2	−2.20	C–H 3.12
					H–H 2.88
(b) Other pollutants					
FA	2.8	−72.5	−31.9	+1.50	C–C 2.83
					O–C 2.82
NH_3	1.6	−60.9	−22.3	+0.71	N–C 3.17
					C–H 2.69

these bonds provided redistribution of the Milliken occupancies in the aromatic groups of MOF by the value of 0.05 e$^-$ per atom. This change in Mulliken occupancies could be the case of minor and visible changes in the stretching frequencies of C–NH_2 bonds and no visible changes in the stretching frequencies of C=C bonds in the aromatic rings (Fig. S9†).

In order to check the validity of this claim, DFT calculations were carried out for DEA and EA molecules as well. Accordingly, EA and DEA molecules were seen to possess mono and di ethyl groups so that they can interact with one and two phenyl rings in the tripod-like cavity of the MOF, respectively. In this respect, the DFT calculations demonstrated a linear relationship between $\Delta H_{(air)}$ and a number of ethylene branches of

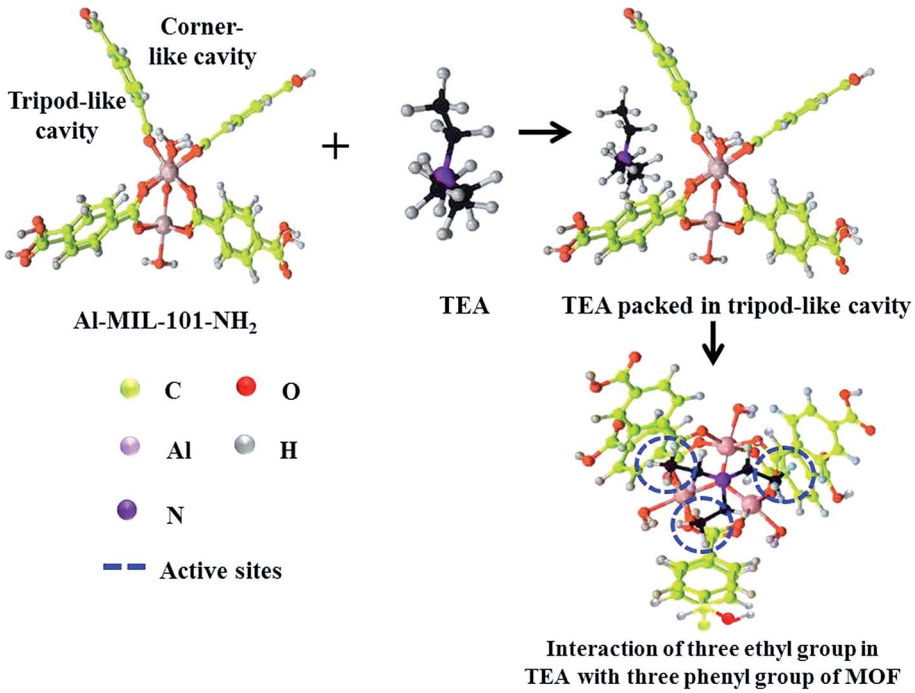

Fig. 3 Sensing mechanism of Al-MOF towards TEA. The carbon atoms of TEA were highlighted with black colour (note: amino groups in the ligand was ignored for clarity).

molecules. For instance, taking into account of adsorption from water and contribution from entropy at RT, obtained lesser negative value of Gibbs free energies for the adsorption of EA (-2.20 kJ mol^{-1}) and DEA (-20.5 kJ mol^{-1}) than that for TEA (-46.7 kJ mol^{-1}) was obtained. This gradual decrease in the ΔG value in relation to decrease in ethylene group confirms the contribution of $-C_2H_5$ group for the enhancement of fluorescence property of Al-MOF. On the other hand, the observed ΔG value for other small molecules such as FA and NH_3 were positive *e.g.*, +1.5 kJ mol^{-1} and +0.71 kJ mol^{-1}, respectively. Thus, it can be concluded that interaction of small molecules (*e.g.*, EA, FA or NH_3) on the linker of Al-MOF was unstable at RT. In addition, the interaction of TEA molecule with MOF was highly stable because it can perfectly fit into the tripod-like cavity and could form stable bond with linker portion of the MOF.

Interaction of guest molecules to open metal sites of MOFs occurred through the formation of coordination bonds which resulted visible changes in the optical properties of both molecule and MOF.[15] In contrast, interaction of molecules on the linkers generated stable van der Waals bond at RT. This weaker bond formation could not change the electronic structure of Al-MOF before and after interaction with TEA molecules (shifts of the peaks were about only 0.02 eV) (Fig. 4) which demonstrated the increasing of intensity of the signal from adsorbed molecule without change in the wavelength (Fig. 1).

The shift of the peaks (about 0.02 eV) was corresponding to the transfer of electrons from MOF to TEA molecule. This electronic transition results the formation of united system, (*e.g.*, Al-MOF–TEA) with common band structure. In addition, the formation of this robust bonds between MOF and TEA led to the appearance of new peaks in valence and conduction bands (peaks 3 and 2*′), respectively (Fig. 4). The appearance of these two new peaks increased the intensity of the adsorption of Al-MOF through a new electronic transitions (3 → 1′, 2′, 2*′,3′, 4 and 1, 2 → 2*′). After adsorption of TEA, these new transitions would help increase the fluorescent emission intensity of Al-MOF (caused by 1′ → 1 transition). Also, the appearance of additional 2*′ peak in conductive band also decreased the probability of radiative transition which result in the transitions

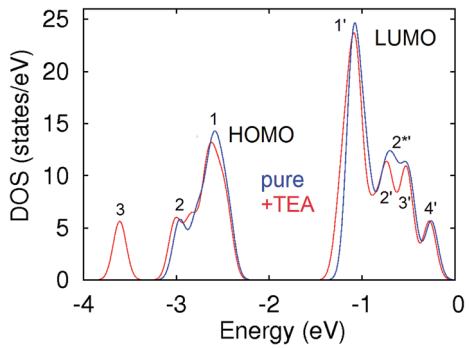

Fig. 4 Total densities of states (DOS) model of Al-MOF before (blue line) and after (red line) adsorption of single TEA molecule in tripod-like cavity. The numbers are corresponding with the important peaks for the optical transitions (see discussions in the text).

of electrons between 4′ and 1′ energy levels. This electronic transition also provided a further enhancement of the fluorescent intensity of Al-MOF–TEA system. Therefore, the formation of the van der Waals bonds between $-CH_3$ groups of TEA and linkers does not affect energetics of stretching of C=C bonds in rings and this in accordance with the obtained FTIR results in the area of 1600–1500 cm^{-1} (Fig. S8†). Therefore, interaction of TEA with Al-MOF was attributed only by decreasing the rotational degrees of freedom of aromatic rings in the linkers and which was majorly supported through van der Waals interaction between the aromatic rings of the MOF with $-C_2H_5$ portions of TEA. These kinds of interactions were not seen in other molecules such as EA and DEA. Overall, this section provides an evidence for the specific sensing of TEA molecule by Al-MOF.

3.7. Recyclability profile of Al-MOF

In an economic viability point of view, a smart material should be recycled and reused for a number of regeneration cycles. To check such possibility, the changes in the sensitivity of the Al-MOF over five regeneration cycles were measured and evaluated (Fig. S11†). The results indicated an excellent recyclability of the proposed probe. In particular, the RFU value of MOF probe solution over five cycles was 259, 256, 254, 249, and 241 a.u, whereas the corresponding fluorescent increment of the probe (at 0.10 mM TEA concentration) was 506, 501, 491, 476, and 462 a.u, respectively. This result clearly supports the inherent stability of the MOF. More importantly, the solvent treatment (water : ethanol) followed by the thermal treatment (150 °C for 1 h) helped enhance the removal of the TEA molecule from the framework structure. This weak force of attraction was also verified by DFT calculation.

4. Conclusions

The structural properties of MOFs act as a critical parameter in the sensing of small molecules especially a molecule like TEA. For instance, TEA molecules possess the lone pair of electrons in nitrogen atoms which act as active sites. These active sites can be used to sense the gaseous TEA through electron migration/generation mechanism. Nonetheless, this kind of mechanism was not common in aqueous phase detection of TEA. As such, the applicability of nanomaterials was limited for sensing aqueous TEA. In light of this drawback, a fluorescent sensor namely Al-MOF was proposed for the sensing of TEA based on lock-and-key mechanism. First of all, the structural properties and aqueous stability of the synthesized Al-MOF was verified with the help of series of characterization, experimental, and DFT calculations. The fluorescent property of Al-MOF was generated by effective charge transfer from ligand to Al^{3+} centres. This charge transfer then increased the Mulliken occupancies of each Al^{3+}centres by 0.29 e$^-$. Also, the examined probe showed enhanced sensitivity for TEA in the concentration range of 0.05–0.99 mM. Fluorescent efficiency of Al-MOF followed linear behaviour in the concentration range of 0.05–0.40 mM with an R^2 value of >0.99. The LOD of the probe was estimated as 3 μM and the probe was found to be exceptionally

selective for the sensing of TEA (ΔG: −46.7 kJ mol^{-1}) over other ethyl amines (ΔG: −2.20 kJ mol^{-1} and size: 3.7 Å) and common industrial pollutants such as formaldehyde (ΔG: +1.50 kJ mol^{-1} and size: 2.8 Å) and ammonia (ΔG: +0.71 kJ mol^{-1} and size: 1.6 Å). DFT calculation brought out the unique fitting between sizes of the TEA molecule with shape of tripod-like cavity in the MOF. This kind of exact fit of TEA in MOF induces a weak C–H interaction between ethyl groups of TEA and the carbon atoms (*i.e.*, π-electrons) of aromatic rings in Al-MOF. This restricts the rotation of aromatic rings in the MOF (*i.e.*, energy cost for the rotation of aromatic rings before and after interaction with TEA was calculated as 5 and 20 kJ mol^{-1}, respectively). In addition, the interaction of TEA with Al-MOF created two new electronic transitions namely 3 → 1′, 2′, 2*′, 3′, 4 and 1, 2 → 2*′ which gradually helped to enhance the fluorescence intensity of the Al-MOF. Overall, this study opened up a new area of research for the sensing of TEA in aqueous solutions.

Conflicts of interest

There are no conflict to declare.

Acknowledgements

The first author KV acknowledges Department of Science and Technology (DST) for providing Nano science and Technology (NST) post-doctoral fellowship (JNC/AO/A.0610(36)2017-2620) and the corresponding author acknowledge Department of Science and Technology (DST), Government of India for providing research funding DST/TN/WTI/WIC/2K17/82.

References

1 T. Koike and M. Akita, *Inorg. Chem. Front.*, 2014, **1**, 562–576.
2 H. S. Pawar, A. S. Wagh and A. M. Lali, *New J. Chem.*, 2016, **40**, 4962–4968.
3 T. Bank, *Hazardous Substances Data*, National Library of Medicine, US, 2011.
4 L.-l. Sui, Y.-M. Xu, X.-F. Zhang, X.-L. Cheng, S. Gao, H. Zhao, Z. Cai and L.-H. Huo, *Sens. Actuators, B*, 2015, **208**, 406–414.
5 Y.-J. Hong, Y.-C. Huang, I.-L. Lee, C.-M. Chiang, C. Lin and H. A. Jeng, *J. Environ. Sci. Health, Part A*, 2015, **50**, 1205–1214.
6 I. Santa Cruz *Biotechnology, Triethylamine: material safety data sheet (no. sc-216008)*, CHEMWATCH, US, 2010.
7 J. Gopalakrishnan and S. A. Devi, *Indian J. Pharm. Sci.*, 2016, **78**, 409–413.
8 C. Seo, J. Yoon, Y. Rhee, J. J. Kim, S. J. Nam, W. Lee, G. Lee, S. T. Yee and M. J. Paik, *Biomed. Chromatogr.*, 2015, **29**, 156–160.
9 M. Manera, E. Ferreiro-Vila, J. García-Martín, A. Cebollada, A. García-Martín, G. Giancane, L. Valli and R. Rella, *Sens. Actuators, B*, 2013, **182**, 232–238.
10 M. Wu, X. Zhang, S. Gao, X. Cheng, Z. Rong, Y. Xu, H. Zhao and L. Huo, *CrystEngComm*, 2013, **15**, 10123–10131.
11 S. Bai, Y. Tian, J. Sun, Z. Tong, R. Luo, D. Li and A. Chen, *New J. Chem.*, 2016, **40**, 4595–4600.
12 P. Li, Y. Zhang, Y. Wang, Y. Wang and H. Li, *Chem. Commun.*, 2014, **50**, 13680–13682.
13 J. Chen, F.-Y. Yi, H. Yu, S. Jiao, G. Pang and Z.-M. Sun, *Chem. Commun.*, 2014, **50**, 10506–10509.
14 K. Vellingiri, A. Deep, K.-H. Kim, D. W. Boukhvalov, P. Kumar and Q. Yao, *Sens. Actuators, B*, 2017, **241**, 938–948.
15 K. Vellingiri, D. W. Boukhvalov, S. K. Pandey, A. Deep and K.-H. Kim, *Sens. Actuators, B*, 2017, **245**, 305–313.
16 K. Vellingiri, J. E. Szulejko, P. Kumar, E. E. Kwon, K.-H. Kim, A. Deep, D. W. Boukhvalov and R. J. Brown, *Sci. Rep.*, 2016, **6**, 27813.
17 S. Liu, Z. Xiang, Z. Hu, X. Zheng and D. Cao, *J. Mater. Chem.*, 2011, **21**, 6649–6653.
18 Y. Xiao, Y. Cui, Q. Zheng, S. Xiang, G. Qian and B. Chen, *Chem. Commun.*, 2010, **46**, 5503–5505.
19 J.-K. Sun and Q. Xu, *Chem. Commun.*, 2014, **50**, 13502–13505.
20 A. Lan, K. Li, H. Wu, D. H. Olson, T. J. Emge, W. Ki, M. Hong and J. Li, *Angew. Chem., Int. Ed.*, 2009, **48**, 2334–2338.
21 Z. Wang, Z. Wang, B. Lin, X. Hu, Y. Wei, C. Zhang, B. An, C. Wang and W. Lin, *ACS Appl. Mater. Interfaces*, 2017, **9**, 35253–35259.
22 M. M. Wanderley, C. Wang, C.-D. Wu and W. Lin, *J. Am. Chem. Soc.*, 2012, **134**, 9050–9053.
23 Y. He, W. Zhou, G. Qian and B. Chen, *Chem. Soc. Rev.*, 2014, **43**, 5657–5678.
24 X.-Y. Xu and B. Yan, *Dalton Trans.*, 2016, **45**, 7078–7084.
25 O. Lebedev, F. Millange, C. Serre, G. Van Tendeloo and G. Férey, *Chem. Mater.*, 2005, **17**, 6525–6527.
26 M. Hartmann and M. Fischer, *Microporous Mesoporous Mater.*, 2012, **164**, 38–43.
27 D. Boukhvalov, V. Y. Osipov, A. Shames, K. Takai, T. Hayashi and T. Enoki, *Carbon*, 2016, **107**, 800–810.
28 K. A. Cychosz and A. J. Matzger, *Langmuir*, 2010, **26**, 17198–17202.
29 J. Yang, Y. Dai, X. Zhu, Z. Wang, Y. Li, Q. Zhuang, J. Shi and J. Gu, *J. Mater. Chem. A*, 2015, **3**, 7445–7452.
30 E. Filippo, D. Manno, A. Buccolieri and A. Serra, *Sens. Actuators, B*, 2013, **178**, 1–9.